Biodegradable and Biocompatible Polyvinyl alcohol/ Silk Fibroin-Based Composite with Improved Strength

XINGMIN XU[1], QINGQING SUN[2], AIRONG XU[2] AND XINBAO GUO[2]

[1] *School of Forensic Medicine, Henan University of Science and Technology, Luoyang, Henan 471000, P. R. China.*

[2] *School of Chemical Engineering & Pharmaceutics, Henan University of Science and Technology, Luoyang, Henan 471000, P. R. China.*

ABSTRACT

Silk fibroin (SF) with renewability, biocompatibility and biodegradability shows potential application in various fields including biomedicine, tissue engineering, and wearable electronic devices. Herein, SF is used to exert effective reinforcement of polyvinyl alcohol (PVA) composite film to further improve its practicability. As such, PVA/SF composite films were prepared for the first time using a facile approach. The films were characterized to investigate possible interaction of PVA with SF. Meanwhile, systematic investigations have also been completed to explore the influences of PVA/SF mass ratio on the mechanical properties (tensile strength, elongation at break), biodegradability and biocompatibility, the morphology, crystallinity, chemical structure and thermostability. It is interesting to find that SF in the PVA/SF can remarkedly exert reinforcement efficacy and improve the mechanical properties, biodegradability and biocompatibility. Due to the reinforcement efficacy of SF, the tensile strength and elongation at break of the PVA/SF material are higher than that of neat PVA material by about 28% and 286%, respectively. Moreover, the materials are biodegradable and biocompatible. The simple and maneuverable approach as well as high-performance properties possessed by the materials will further broaden their practical application.

KEYWORDS: *Silk fibroin, Polyvinyl alcohol composite film, Effective reinforcement, Mechanical properties, Biodegradability and Biocompatibility.*

J. Polym. Mater. Vol. **39,** No. 1-2, 2022, 167-181

Correspondence author e-mail: airongxu@haust.edu.cn
DOI : https://doi.org/10.32381/JPM.2022.39.1-2.11

INTRODUCTION

With the increasing needs to develop environmentally friendly alternatives to petroleum-derived products which are generally nonbiodegradable and pollute human survival environment, green and biodegradable products which are prepared from nontoxic biodegradable synthetic polymers (polyvinyl alcohol (PVA), polylactic acid (PLA), poly (D, L-lactide-co-glycolide) (PLGA), poly(1,4-butylene succinate) (PBS), and so on) or sustainable biomass polymer (silk fibroin, cellulose, lignin and starch, and the like) have attracted great attention in both academy and industry[1-6]. Among the nontoxic biodegradable polymers, PVA has received wide attention due to its fascinating properties such as biocompatibility, film forming, biodegradability, low friction factor and permeability[7-9].

Based on its compelling advantages, significant efforts have been made to use PVA for fabricating eco-friendly and biodegradable products in plastic packaging field in recent years [1]. However, neat PVA can hardly be used to be directly processed into desired product, especially film product because of its poor mechanical property and water-retention property [10,11]. To overcome these disadvantages, many attempts have been made to combine additional feedstock with PVA. Among a variety of additives, green and renewable biomass has been the hot spot of the current research under the background of the attempt of the alternatives to petroleum-derived products. For example, Okahisa et al. found that cellulose nanofiber from oil palm tree could improve the tensile strength and Young's modulus as well as thermal stability of the PVA/cellulose nanofiber film [12]. Similar findings have been reported for the reinforcement of the PVA/cellulose nanofiber materials using cellulose nanofibers from oil palm empty fruit bunches, rice straw and coconut coir fibers [13-15]. In addition, cellulose nanocrystal derived from microcrystalline cellulose could reinforce polyvinyl alcohol composite film in which PVA was modified by maleic anhydride [16].

Although cellulose nanofiber and nanocrystal possess excellent features, the involvement of chemicals and complexity in extraction process limits their usage [16-18]. Moreover, these PVA nanocomposites are generally brittle and not ductile [12,16]. In recent years, starch, another biomass, has been investigated to be combined with PVA to prepare PVA/starch films [19-21]. However, the tensile strength and elongation at break of PVA/starch films are apparently less than those of neat PVA film. Therefore, starch cannot improve the mechanical properties of the PVA/starch films due to its brittle nature.

Silk fibroin (SF), another abundantly available and reasonable cost biomass, produced from *Bombyx mori* cocoons, shows remarkable mechanical properties, controllable degradation rates, biocompatibility and low immunogenicity[22-25]. It has been extensively applied in not only traditional textile industry but also biomedical and separation fields [23-30]. At the same time, SF can be constructed into varying forms including sponges, scaffolds, particles, fibres, films and hydrogels [30-33]. Moreover, it can also be as a reinforcing agent to improve the mechanical properties of a composite [34]. Assuming that SF and PVA are introduced into the same phase, it is likely that this PVA/SF can be prepared with improved properties and applicability.

Therefore, in this study, SF was employed as a reinforcing agent to be introduced into PVA to prepare PVA/SF composite films. Further, SEM (scanning electron microscope), XRD (X-ray diffraction), IR (infrared spectroscopy) and TGA (thermogravimetric analysis) techniques were employed to investigate the microstructure, crystalline state, thermostability of these films and possible interaction of PVA with SF. At the same time, systematic investigations have been achieved to reveal the influences of PVA/SF mass ratio on the mechanical properties (tensile strength, elongation at break), biodegradability and biocompatibility, the morphology, crystallinity, chemical structure and thermostability.

EXPERIMENTAL

Materials

Dialysis bag (8000-14000) was purchased from Shanghai Yuanye Biotechnology Co., Ltd. Silk cocoon (*Bombix mori*) was purchased from Jiangsu Haian Xichang Reeling Silk Co., Ltd. Hexafluoroisopropanol (HFIP) and polyvinyl alcohol (PVA) (Mw, 145000) were purchased from Aladdin Biochemical Technology Co., Ltd. Both DMEM medium and MTT were purchased from Beijing Solable Technology Co., Ltd. Fetal bovine serum was purchased from Zhejiang Tianhang Biotechnology Co., Ltd. Phosphorus pentoxide was purchased from Tianjin Hengxing Chemical Reagent Co., Ltd.

Preparation of Silk Fibroin

Silk fibroin was prepared by using a similar procedure described in the literature [35,36]. The silk cocoon was degummed three times by boiling it in 0.5 wt.% Na_2CO_3 aqueous solution for 30 min followed by washing with deionized water and drying at room temperatures. The degummed silk cocoon was named as silk fibroin (SF). The SF was dissolved in ternary solution $CaCl_2$-CH_3CH_2OH-H_2O (molar ratio of 1:2:8) at 70°C ~ 80°C to obtain mixture solution. The mixture solution was filtered with a glass funnel lined with filter paper, and the filtrate in dialysis bag was dialysed in deionized water for 3 days. The dialyzed SF aqueous solution was freeze-dried to obtain the white SF.

Preparation of the PVA/SF Composite Film

The PVA/SF composites were prepared as follows. The PVA/SF/HFIP solution was prepared by dissolving PVA and SF in HFIP at 50°C. The total concentration of PVA and SF in HFIP was about 1.5 wt.%. The flask containing the PVA/SF/HFIP solution was put in a ultrasonic apparatus for about 30 min to desecrate the bubbles. Then, the PVA/SF/HFIP solution was poured into a glass mold (10 cm × 10 cm). A PVA/SF film was obtained after HFIP volatilization. The resultant PVA/SF film was dried in vacuum oven for at 50°C for the complete evaporation of HFIP residual at the presence of P_2O_5. The obtained composite film is coded as PVA/SF(x:y), and x:y represents the mass ratio of PVA to SF.

Characterization of the PVA/SF Composite Film

Scanning electron micrograph (SEM) measurements were photographed on a FLEXSEM 1000 scanning electron microscope. The dry PVA/SF film was frozen by liquid nitrogen and snapped directly. After being sputtered by gold, the fracture surfaces were photographed.

Fourier transform infrared (FTIR) measurements were reported on an ATR-FTIR (Nicolet iN10, Thermo Fisher Scientific, USA) system with Ge crystal ATR accessory with a total of 64 scans and a resolution of 4 cm^{-1}. A NETZSCH STA 449 C thermal analyzer was used for thermogravimetric analysis (TGA) using alumina crucibles under flowing nitrogen gas atmosphere at a heating rate of 10°C per minute. X-ray diffraction (XRD) measurements were collected on a Bruker D8 Advance diffraction spectrometer with Cu-Ka radiation (λ = 1.54 Å) at 40 kV and 30 mA over the range 5–60° (2θ) at a scan speed of 2°C per minute.

Mechanical Property Measurements of the PVA/SF Composite Film

Sample film was cut into dumbbell-shaped specimen of 75 mm length and then kept in a dryer with saturated NaCl solution (RH = 75%) for 24 h. elongations at break and elongation at break measurements were performed on a WDW-10 universal tensile tester according to ISO

527-3, 1995 (E) with an extension rate of 2 mm min^{-1} and gauge length of 20 mm. Tensile strength and elongation at break values were averages of five measurements.

Soil Biodegradation Measurements of the PVA/SF Composite Film

To investigate the biodegradation of the PVA/SF composite film. Each film sample (3×3 cm^2) enclosed in a nylon mesh netting (2×2 mm^2 mesh size) was buried in about 15 cm beneath natural soil on our campus. The soil was watered once a day (except on rainy days) to ensure that the experimental soil was always wet. The biodegradation time lasted from May to July.

Each degraded film was taken from the soil, washed with deionized water to remove the soil on the surface of the membrane, and lyophilized to a constant weight. The degradation efficiency was calculated using equation (1).

$$\text{Degradation efficiency (\%)} = (M_o - M_d)/M_o \times 100 \quad (1)$$

In equation (1), M_o and M_d are the weight of the membrane before and after degradation, respectively.

In Vitro Cell Assay

The standard MTT assay was used to estimate the viability of EC109 cells on the PVA/SF membrane. The membrane was flatly laid on the bottom of a well of a 96-well plate and sterilized by autoclaving. The EC109 cells were seeded on the membrane at a density of 5000 cells/well, and 100 μL DMEM containing 10% FBS (fetal bovine serum) was added to the well. The EC109 cells were allowed to grow in a incubator at 37°C in a 5 vol% CO_2 atmosphere for 24 h.

After incubating for 24 h, 20 μL MTT (5 mg/mL in PBS buffer) solution was added into each well and incubated for another 4 h. Finally, the medium was replaced with 200 μL DMSO. The absorbance was measured at 570 nm by a microplate reader (Bio-Rad, Model 550, USA). For each sample, at least six parallel experiments were conducted, and the average value was used. The relative cell viability was assessed using the following equation:

$$\text{Cell viability (\%)} = (A_{test}\,(\text{sample})/A_{control}(\text{control})) \times 100 \quad (2)$$

where A_{test} and $A_{control}$ are the absorbance values of the test and control groups, respectively.

RESULTS AND DISCUSSION

Morphology of the PVA/SF Composite

The SEM images of the fracture surfaces of the neat PVA film and PVA/SF composite films are shown in Figure 1. The neat PVA material exhibits a dense and smooth morphology with very few PVA microspheres (see circle in Figure 1a), indicating that some PVA macromolecules can agglomerate into microspheres even in the neat PVA material. Over the PVA/SF mass ratio range of 90:10 to 50:50, remarkable phase separation can be observed (Figures 1b-d). The PVA/SF (90:10) composite shows a dense and smooth morphology similar to the neat PVA material. However, there are much more PVA microspheres in the PVA/SF (90:10) composite than in the neat PVA material (Figures 1b). Moreover, with increasing PVA/SF mass ratio from 90:10 to 50:50, more and bigger PVA microspheres can be observed in the composite. At the same time, it is found that with a further increase in SF content, PVA microspheres becomes less and lessens (Figures 1e-f). The above findings indicate that when SF content is ≤ 10 wt.% or ≥ 70 wt.%, the phase separation of PVA with SF is less apparent, and the PVA microspheres in the composites show small sizes. On the other hand, when SF content ranges 30-50 wt.%, the composites show apparent phase separation, and big PVA microspheres can be observed. This is mainly ascribed to the facts that when SF content is ≤ 10 wt.%, PVA can agglomerate into smaller microspheres like the neat PVA material; when SF content is ≥ 70 wt.%, PVA can also agglomerate into smaller microspheres due to a small number of PVA; when SF content ranges 30-50 wt.%, PVA can agglomerate into bigger microspheres due to

a large number of PVA. In addition, the above findings also indicate that PVA heterogeneously hybridizes with SF.

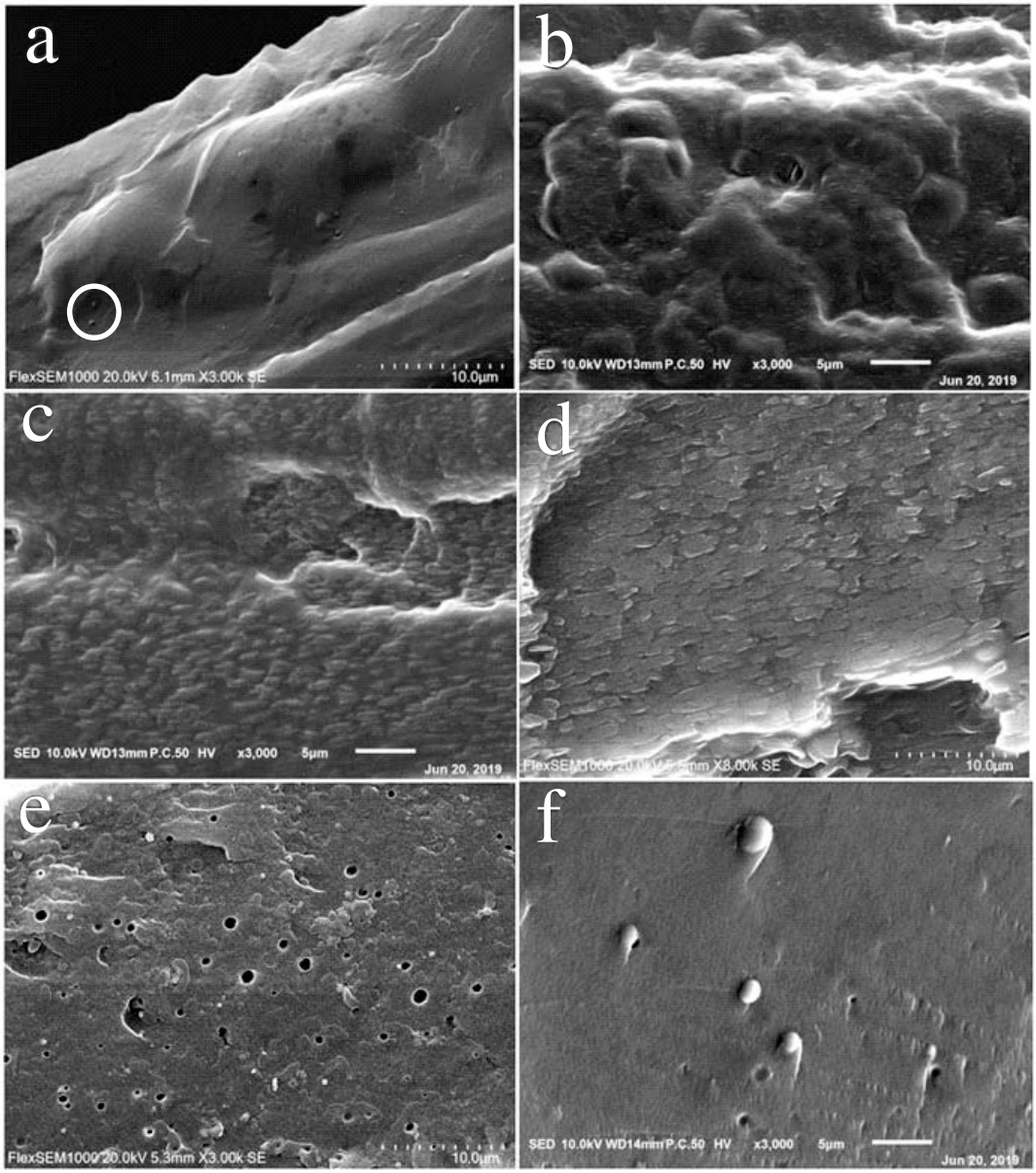

Fig. 1. SEM images: (a) PVA film; (b) PVA/SF(90:10), (c) PVA/SF(70:30), (d) PVA/SF(50:50), (e) PVA/SF(30:70), (f) PVA/SF(10:90) composite films.

XRD, TGA and IR Analysis of the PVA/SF Composite

The XRD diffraction patterns of PVA film, PVA/SF composite films and SF film are shown in Figure 2. SF shows an amorphous state, and thus no diffraction peak is observed. The typical XRD diffraction peak at $2\theta = 19.6°$ for PVA can be observed in the PVA/SF (90:10), PVA/SF (70:30), PVA/SF (50:50) and PVA/SF (30:70) composites[12]. Moreover, the higher the content of PVA, the stronger the intensity of the peak of PVA. This indicates that PVA in the composites still retains the same crystalline state with original PVA. At the same time, this also reveals that the hybridization of PVA with SF is heterogeneous, which is in good agreement with the SEM results.

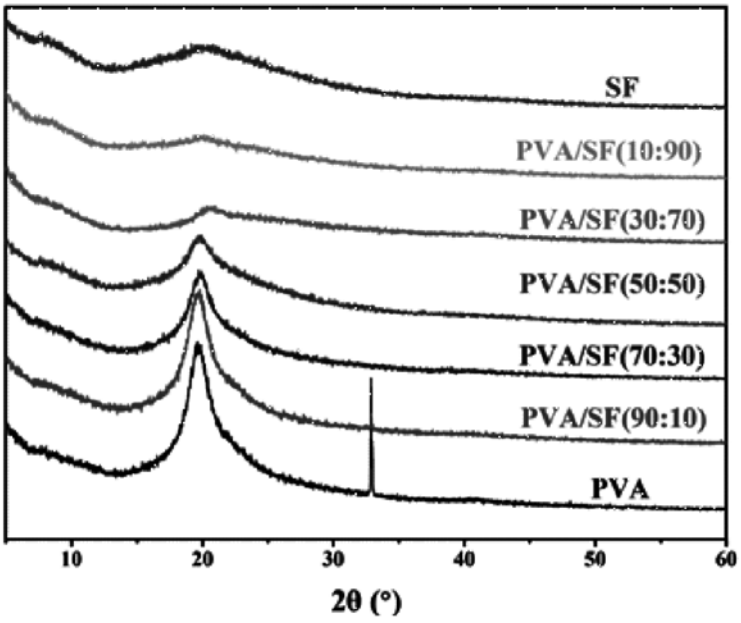

Fig. 2. XRD patterns: PVA, PVA/SF and SF films. The diffraction peak at 33.1° was ascribed to the glass substrate on which PVA powder was placed.

As shown in Figure 3, the decomposition temperature of PVA is 296°C, 278°C for the PVA/SF (50:50) composite, and 262°C for SF, respectively. Therefore, after PVA hybridizes with SF, the decomposition temperatures of the PVA/SF composites are higher that of SF and lower than that of PVA. The composites still possess good thermal stability. It is also found that the TGA curve of the PVA/SF (50:50) sample shows two weight loss platforms relative to PVA and SF, respectively. This indicates a heterogeneous composite of PVA with SF, which is in good agreement with the SEM and XRD results.

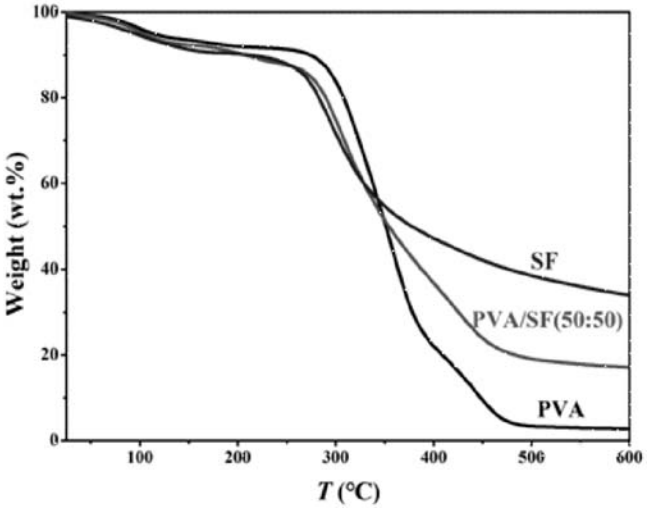

Fig. 3. TGA curves: PVA, PVA/SF(50:50) and SF films

Figure 4 summarizes the IR spectra of PVA, PVA/SF composites and SF. The typical peak at 3310 cm^{-1} is ascribed to the O–H stretching of PVA [12]. The typical peaks at 3287 cm^{-1} and 1651 cm^{-1} are associated with the N–H stretching vibration and C=O carbonyl stretching vibration of SF, respectively [24]. In the PVA/SF composite, with an increase in SF, on one hand, the peaks corresponding to PVA gradually weaken; on the other hand, the

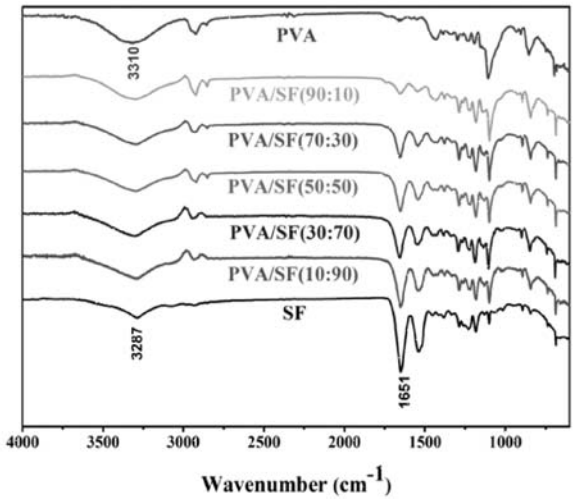

Fig. 4. FT-IR spectra: PVA film, PVA/SF composite films and SF film

peaks corresponding to SF gradually strengthen. Moreover, the wavenumbers associated with PVA and SF retain almost unchanged. This suggests that PVA hardly interacts with SF. This also reveals a heterogeneous composite of PVA with SF, which is in accordance with the SEM, XRD and TGA findings.

Biodegradation and Cell Viability of the PVA/SF Composite

PVA and SF have been extensively recognized as biodegradable polymers [7, 22]. However, little is still known about the biodegradation behavior of the PVA/SF composite. Therefore, the degradation efficiency of the PVA/SF composite in soil was determined as a function of time (day) (Figure 5). By comparison, neat PVA exhibits very low degradation efficiency, and only 12% of degradation efficiency is obtained after 90 days. Interestingly, after the hybridization of PVA with SF, the PVA/SF composite becomes more biodegradable, and the degradation efficiency considerably increases with increasing SF content. For example, after 90 day of biodegradation in soil, the degradation efficiencies of the PVA/SF composites remarkedly increase in the order PVA (12%) < PVA/SF(10:90) (17%) < PVA/SF(70:30) (32%) < PVA/SF(50:50) (50%) < PVA/SF(70:30) (70%) < PVA/SF(90:10) (95%). Therefore, SF can significantly accelerate the biodegradation the PVA/SF composite. This can be rationalized based on the following fact that the neat PVA film exists in crystalline state (see Figure 2), its macromolecule chains were densely bound together due to the interaction of the CH_2CH_2 chains and hydrogen bonds between PVA molecular chains. Hence, water molecules and

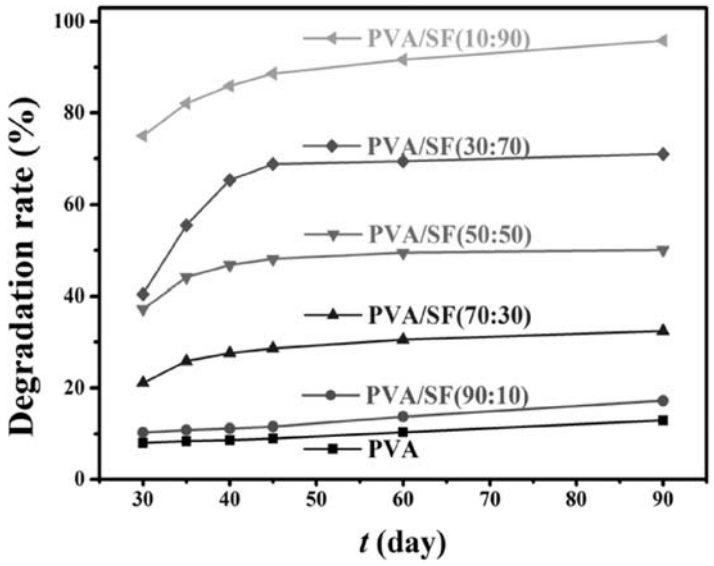

Fig. 5. Degradation efficiency (%) vs. burial time (day) for neat PVA and PVA/SF composite membranes

bacteria were difficult to penetrate into the chains for the hydrolysis or degradation of PVA under soil-buried conditions. In contrast, after the hybridization of PVA with SF, PVA crystallinity in the PVA/SF composite is decreased (see Figure 2). This provides great possibility for the entrance of water molecules, bacteria, microorganisms and fungi from the soil into the PVA/SF film and thus its degradation.

SEM technique was used to observe the morphology of neat PVA, PVA/SF (90:10), PVA/SF (70:30) and PVA/SF (50:50) composites after 30, 60 and 90 days of burying in soil (Figure 6). The corrosions of the surfaces of all the films are apparently observable, and become increasingly severe with burial time and SF content. Therefore, the PVA/SF composites are environmentally degradable and can be employed as friendly materials.

Importantly, unlike conventional polymer materials such as polyethylene and polypropylene which require hundreds or even thousands of years to degrade [37]. The PVA/SF materials in this work were fabricated using renewable and/or nontoxic PVA and SF. These materials exhibit

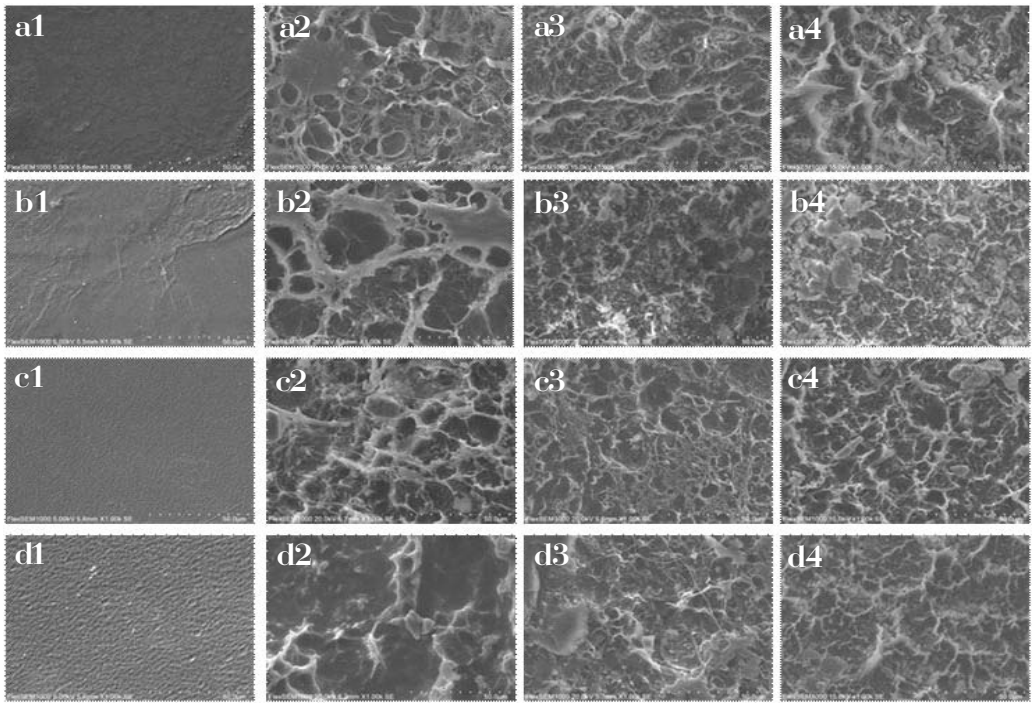

Fig. 6. SEM images: neat PVA: before degradation (a1), degradation for 30 days (a2), degradation for 60 days (a3), degradation for 90 days (a4); PVA/SF (90:10) composite film: before degradation (b1), degradation for 30 days (b2), degradation for 60 days (b3), degradation for 90 days (b4); PVA/SF (70:30) composite film: before degradation (c1), degradation for 30 days (c2), degradation for 60 days (c3), degradation for 90 days (c4); PVA/SF (50:50) composite film: before degradation (d1), degradation for 30 days (d2), degradation for 60 days (d3), degradation for 90 days (d4).

good biodegradability, and thus meeting environmentally friendly requirements advocated by green chemistry.

The values of cell viability were used to evaluate the EC109 cell response on the PVA/SF composites (Figure 7). For all the samples including neat PVA, the PVA/SF composites and neat SF, the values of cell viability are higher than 100%. This suggests that these materials are nontoxic and biocompatible in terms of cell responses, and thus can be applied in biomedical fields as potential biomaterials. It is also found that the cell viability on the PVA/SF composites increases with a slight increase in SF content. This indicates that the hybridization of PVA with SF is beneficial to the growth and proliferation of the EC109 cells.

The above investigations reveal that the PVA/SF composite developed in this work can be employed as a potential and green alternative to conventional and nondegradable polyethylene and polypropylene materials because of its biodegradability, biocompatibility, nontoxicity, and so on.

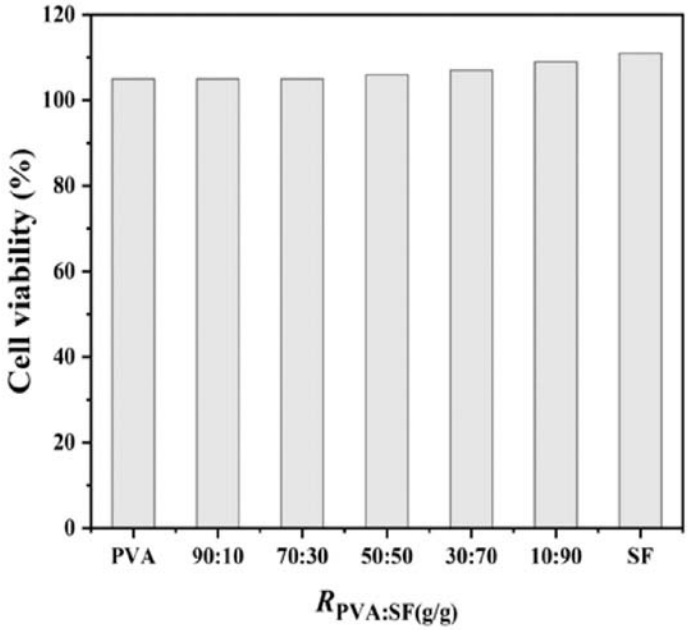

Fig. 7. Cell viability (%) for the PVA/SF composites

Tensile Properties of the PVA/SF Composite

When PVA/SF mass ratio is less than 50:50 (SF content in the PVA/SF composites is higher than 50%), the PVA/SF membrane is too fragile to perform the experiments of tensile properties (tensile strength of elongations at break), and similarly for neat SF. Therefore, the experiments of the tensile properties were completed at the mass ratio range of from 100:0 to 50:50.

The tensile strengths of the neat PVA and PVA/SF composite films are given in Figure 8. The tensile strength of the PVA/SF film is remarkedly impacted by PVA/SF mass ratio. The tensile strength of the PVA/SF film enhances in the order PVA (32 MPa) < PVA/SF (97:3) (33 MPa) < PVA/SF (95:5) (35 MPa) < PVA/SF (90:10) (38 MPa) < PVA/SF(70:30) (43 MPa). The PVA/SF composite film shows the maximum tensile strength (43 MPa) at RPVA:SF = 70:30, and then reduces. Therefore, SF can enhance the tensile strength of the PVA/SF composite. This is mainly due to increased interfacial adhesion. At the same time, it is found that when the PVA/SF mass ratio is less than 50:50, the tensile strength is dramatically reduced. This primarily attributes to the fact that the higher SF content is in the PVA/SF composite, the more fragile the composite is, causing a decrease in tensile strength.

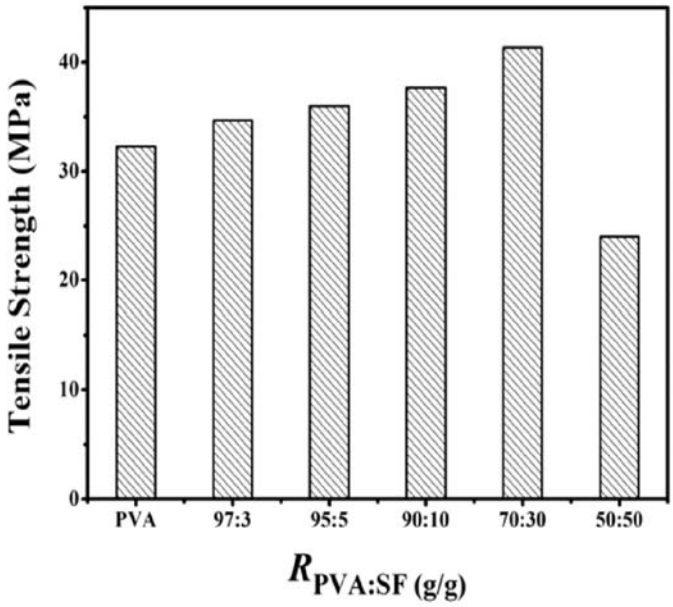

Fig. 8. Tensile strength of neat PVA and PVA/SF composite membranes

The elongations at break of the neat PVA and PVA/SF membranes are given in Figure 9. The elongations at break are also impacted by PVA/SF mass ratio. The elongations at break of the PVA/SF membrane enhances in the order PVA (85 %) < PVA/SF (97:3) (130 %) < PVA/SF (95:5) (154 %). The PVA/SF composite membrane shows the maximum elongation at break (154%) at $R_{PVA:SF}$ = 95:5, and then reduced. Therefore, SF can also enhance the elongations at break of the PVA/SF composite. It is also noted that when the PVA/SF mass ratio is less than 90:10, the elongations at break is significantly reduced. This is mainly ascribed to the fragility of SF.

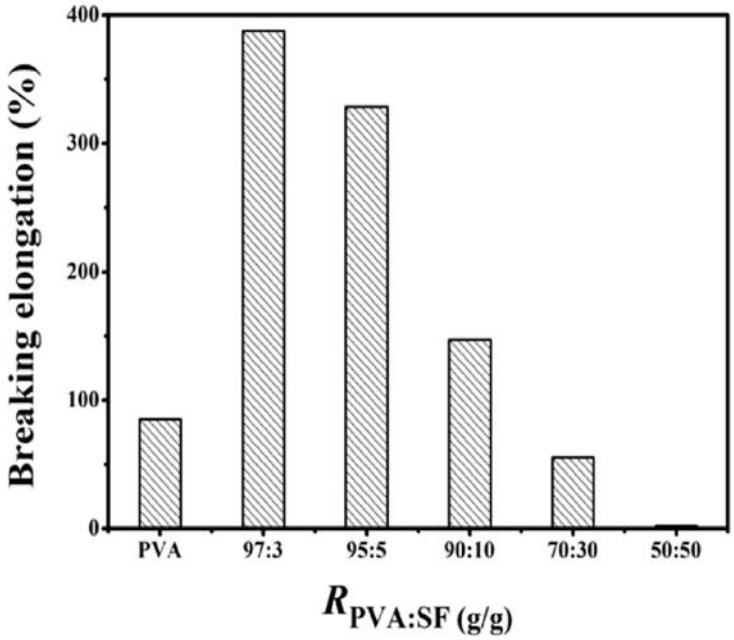

Fig. 9. The elongations at break of neat PVA and PVA/SF composite membranes

CONCLUSION

In the present wok, a facible strategy has been developed to construct the PVA/SF composites with high performance. The degradation efficiency, biocompatibility, tensile strength and elongation at break of the composite strongly depend on the PVA/SF mass ratio. Proper PVA/SF mass ratios can remarkedly enhance degradation efficiency, biocompatibility, tensile strength and elongation at break. Compared with neat PVA membrane, the degradation efficiency is enhanced by about 14% after 90 days of burying in soil, the tensile strengths of the PVA/SF (100:0 – 70:30) composites are improved by about 6 –28%, and the elongations at break are increased by about 73–286% at $R_{PVA:SF}$ = 100:0 – 90:10. Meanwhile, the PVA/SF composites show excellent biocompatibility and cell proliferation. Additionally, XRD, IR, SEM and TGA findings reveal that the crystallinity of PVA in the PVA/SF composite is reduced, the PVA/SF composites exhibit dense morphologies with aggregated spheres, PVA physically composites with SF, and the composites show good thermostability.

Acknowledgments

The authors are grateful to the Natural Science Foundation of Henan Province (222300420432, 182300410168) and SRTP Program, Henan University of Science and Technology (2022186).

Author Contributions

Xingmin Xu and Qingqing Sun contributed equally to this work.

Conflict of Interest

The authors declare no conflict of interest.

References

1. Kumar S, Singh P, Gupta SK, Ali J, Baboota S (2020). Biodegradable and recyclable packaging materials: a step towards a greener future. *Encyclopedia of Renewable and Sustainable Mater,* 5: 328-337. https://doi.org/10.1016/B978-0-12-803581-8.10934-8
2. Kirillova A, Yeazel TR, Asheghali D, Petersen SR, Dort S, Gall K, Becker ML (2021). Fabrication of biomedical scaffolds using biodegradable polymers. *Chem Rev,* 121: 11238-11304. https://doi.org/10.1021/acs.chemrev.0c01200
3. Tripathi N, Misra M, Mohanty AK (2021). Durable polylactic acid (pla)-based sustainable engineered blends and biocomposites: recent developments, challenges, and opportunities. *ACS Eng Au,* 1: 7-38. https://doi.org/10.1021/acsengineeringau.1c00011
4. Wu F, Misra M, Mohanty AK (2021). Challenges and new opportunities on barrier performance of biodegradable polymers for sustainable packaging. *Prog Polym Sci,* 117: 101395. https://doi.org/101395. 10.1016/j.progpolymsci.
5. Sheldon RA, Norton M (2020). Green chemistry and the plastic pollution challenge: towards a circular economy. *Green Chem,* 22:6310-6322. https://doi.org/10.1039/D0GC02630A
6. Jagadeesh P, Puttegowda M, Rangappa SM, Siengchin S (2021). Influence of nanofillers on biodegradable composites: a comprehensive review. *Polym Composite,* 42: 5691. https://doi.org/10.1002/pc.26291.
7. Zhang S, Li Y, Zhang H, Wang G, Wei H, Zhang X, Ma N (2021). Bioinspired conductive hydrogel with ultrahigh toughness and stable antiswelling properties for articular cartilage replacement. *ACS Mater Lett,* 3: 807. https://doi.org/10.1021/acsmaterialslett.1c00203.
8. Zhang S, Zhang Y, Li B, Zhang P, Kan L, Wang G, Wei H, Zhang X, Ma N (2019) One-step preparation of a highly stretchable, conductive, and transparent poly (vinyl alcohol)–phytic acid hydrogel for casual writing circuits. *ACS Appl Mater Inter,* 11:32441. https://doi.org/10.1021 acsami.9b12626.
9. Wen J, Tang J, Ning H, Hu N, Zhu Y, Gong Y, Xu C, Zhao Q, Jiang X, Hu X, Lei L, Wu D, Huang T (2021). Multifunctional ionic skin with sensing, UV-filtering, water-retaining, and anti-freezing capabilities. *Adv Funct Mater,* 31: 91117617. http://doi.org/10.1002/adfm.202011176.
10. Jiang SD, Tang G, Bai ZM, Wang YY, Hu Y, Song L (2014). Surface functionalization of MoS 2 with POSS for enhancing thermal, flame-retardant and mechanical properties in PVA composites. *RSC Adv,* 4: 3253. http://doi.org/10.1039/C3RA45911J.
11. Shuai C, Feng P, Gao C, Shuai X, Xiao T, Peng S (2015). Graphene oxide reinforced poly(vinyl alcohol): nanocomposite scaffolds for tissue engineering applications. *RSC Adv,* 5: 25416-25423. https://doi.org/10.1039/C4RA16702C.
12. Okahisa Y, Matsuoka K, Yamada K, Wataoka I (2020). Comparison of polyvinyl alcohol films reinforced with cellulose nanofibers derived from oil palm by impregnating and casting methods. *Carbohyd Polym,* 250: 116907. https://doi.org/10.1016/j.carbpol.2020.116907.
13. Fahma F, Hori N, Iwata T, Takemura A (2017). PVA nanocomposites reinforced with cellulose nanofibers from oil palm empty fruit bunches (OPEFBS). *Emir J Food Agr,* 29: 1. https://doi.org/10.9755/ejfa.2016-02-215.
14. Wang Z, Qiao X, Sun K (2018). Rice straw cellulose nanofibrils reinforced poly (vinyl alcohol) composite films. *Carbohyd Polym,* 197: 442-450. https://doi.org/10.1016/j.carbpol.2018.06.025.
15. Wu J, Du X, Yin Z, Xu S, Xu S, Zhang Y (2019). Preparation and characterization of cellulose nanofibrils from coconut coir fibers and their reinforcements in biodegradable composite films. *Carbohyd Polym,* 211: 49. https://doi.org/10.1016/j.carbpol.2019.01.093.

16. Song M, Yu H, Gu J, Ye S, Zhou Y (2018). Chemical cross-linked polyvinyl alcohol/cellulose nanocrystal composite films with high structural stability by spraying Fenton reagent as initiator. *Int J Biol Macromol,* 113:171. https://doi.org/10.1016/j.ijbiomac.2018.02.117.

17. Menon MP, Selvakumar R, Suresh kumar P, Ramakrishna S (2017). Extraction and modification of cellulose nanofibers derived from biomass for environmental application. RSC Adv 7: 42750-42773. https://doi.org/10.1039/C7RA06713E.

18. Siró I, Plackett D (2010). Microfibrillated cellulose and new nanocomposite materials: a 403 review. *Cellulose,* 17: 459-494. https://doi.org/10.1007/s10570-010-9405-y.

19. Afzal A, Khaliq Z, Ahmad S, Ahmad F, Noor A, Qadir MB (2021). Development and characterization of biodegradable composite film. *Environ Technol Inno,* 23: 101664. https://doi.org/10.1016/j.eti.2021.101664.

20. Patil S, Bharimalla AK, Mahapatra A, Lad JD, Arputharaj A, Kumar M, Raja ASM, Kambli N (2021). Effect of polymer blending on mechanical and barrier properties of starch-polyvinyl alcohol based biodegradable composite films. *Food Biosci* 44: 101352. https://doi.org/10.1016/j.fbio.2021.101352

21. Hilmi FF, Wahit MU, Shukri NA, Ghazali Z, Zanuri AZ (2019). Physico-chemical properties of biodegradable films of polyvinyl alcohol/sago starch for food packaging. Mater Today: Proceedings 16: 1819-1824. https://doi.org/10.1016/j.matpr.2019.06.056

22. Kundu J, Poole-Warren LA, Martens P, Kundu SC (2012). Silk fibroin/poly(vinyl alcohol) photocrosslinked hydrogels for delivery of macromolecular drugs. Acta Biomater 8: 1720-1729. https://doi.org/10.1016/j.actbio.2012.01.004.

23. Yao Y, Mukuze KS, Zhang Y, Wang H (2014). Rheological behavior of cellulose/silk fibroin blend solutions with ionic liquid as solvent. *Cellulose* 21: 675-84. https://doi.org/10.1007/s10570-013-0117-y.

24. Nourmohammadi J, Roshanfar F, Farokhi M, Nazarpak MH (2017). Silk fibroin/kappa-carrageenan composite scaffolds with enhanced biomimetic mineralization for bone regeneration applications. *Mat Sci Eng C,* 76:951-958. https://doi.org/10.1016/j.msec.2017.03.166.

25. Mottaghitalab F, Hosseinkhani H, Shokrgozar MA, Mao C, Yang M, Farokhi M (2015). Silk as a potential candidate for bone tissue engineering. *J Control Release,* 215: 112-128. https://doi.org/10.1016/j.jconrel.2015.07.031.

26. Zhang C, Zhang Y, Shao H, Hu X (2016). Hybrid silk fibers dry-spun from regenerated silk fibroin/graphene oxide aqueous solutions. *ACS Appl Mater Inter,* 8: 3349-3358. https://doi.org/10.1021/acsami.5b11245.

27. Shang S, Zhu L, Fan J (2011). Physical properties of silk fibroin/cellulose blend films regenerated from the hydrophilic ionic liquid. *Carbohyd Polym,* 86: 462-468. https://doi.org/10.1016/j.carbpol.2011.04.064.

28. Wenk E, Merkle HP, Meinel L (2011) Silk fibroin as a vehicle for drug delivery applications. *J Control Release,* 150: 128-141. https://doi.org/10.1016/j.jconrel.2010.11.007.

29. Mandal BB, Park SH, Gil ES, Kaplan DL (2011). Multilayered silk scaffolds for meniscus tissue engineering. *Biomaterials,* 32: 639-651. https://doi.org/10.1016/j.biomaterials.2010.08.115.

30. Ling S, Jin K, Kaplan DL, Buehler MJ (2016). Ultrathin free-standing bombyx mori silk nanofibril membranes. *Nano Lett,* 16: 3795-3800. https://doi.org/10.1021/acs.nanolett.6b01195.

31. Vepari C, Kaplan DL (2007). Silk as a biomaterial. *Prog Polym Sci,* 32: 991-1007. https:// 443 doi.org/10.1016/j.progpolymsci.2007.05.013.

32. Zheng H, Zuo B (2021). Functional silk fibroin hydrogels: preparation, properties and applications. *J Mater Chem B,* 9: 1238-1258. https://doi.org/10.1039/D0TB02099K.

33. Zuluaga-Vélez A, Quintero-Martinez A, Orozco LM, Sepúlveda-Arias JC (2021) Silk fibroin

nanocomposites as tissue engineering scaffolds-A systematic review. Biomed Pharmacother 141: 111924. https://doi.org/10.1016/j.biopha.2021.111924.

34. Zheng H, Lin N, He Y, Zuo B (2021). Self-healing, self-adhesive silk fibroin conductive hydrogel as a flexible strain sensor. *ACS Appl Mater Inter,* 13: 40013-40031. https://doi.org/10.1021/acsami.1c08395.

35. Pan H, Zhang Y, Hang Y, Shao H, Hu X, Xu Y, Feng C (2012). Significantly reinforced composite fibers electrospun from silk fibroin/carbon nanotube aqueous solutions. *Biomacromolecules,* 13: 2859-2867. https://doi.org/10.1021/bm300877d.

36. Shayannia M, Sajjadi H, Motaghitalab V, Haghi AK (2017). Effect of multi wall carbon nanotubes on characteristics and morphology of nanofiber scaffolds composited of MWNTs/silk fibroin. *Adv Powder Technol,* 28: 775-784. https://doi.org/10.1016/j.apt.2016.11.025.

37. Alimuzzaman S, Gong RH, Akonda M (2014). Nonwoven polylactic acid and flax biocomposites. *Polym Composite,* 35: 2094-2012. https://doi.org/10.1002/pc.22561.

Received: 29-01-2021

Accepted: 08-04-2022